

Assessment of active tectonics from geomorphic indices and morphometric parameters in part of Ganga basin

Aditya Kumar ANAND  <https://orcid.org/0000-0001-7899-9086>; e-mail: aditya.erri@gmail.com

Sarada Prasad PRADHAN*  <https://orcid.org/0000-0001-5054-4370>;  e-mail: saradaiitb@gmail.com

* Corresponding author

Department of Earth Sciences, Indian Institute of Technology Roorkee, Roorkee-247667, India

Citation: Anand AK, Pradhan SP (2019) Assessment of active tectonics from geomorphic indices and morphometric parameters in part of Ganga basin. Journal of Mountain Science 16(8). <https://doi.org/10.1007/s11629-018-5172-2>

© Science Press, Institute of Mountain Hazards and Environment, CAS and Springer-Verlag GmbH Germany, part of Springer Nature 2019

Abstract: Ganga river basins exposed to active erosional and deformational processes. The recurrence of landslides, floods, and seismic activities makes it more susceptible to deformational activities. The tectonic analysis using geomorphic indices and morphometric parameters will help in determining the hazard-prone area of the river basin. Geomorphic indices and morphometric parameters are calculated to investigate the role of neotectonic activities, as it acts as a controlling factor in the development of landforms in the tectonically active terrains. Neotectonic activities influence the terrain topography, which significantly affects the drainage system and geomorphological setup of the area. In this study, the assessment of active tectonics of study area was determined using Advanced Spaceborne Thermal Emission and Reflection Radiometer (ASTER) Global Digital Elevation Model (GDEM) based on Geomorphic Indices (Stream Length Gradient index, Hypsometric integral, Asymmetry factor, Basin shape, Valley floor width to Valley height ratio, Mountain front sinuosity index) cumulatively with Linear, Areal and Relief morphometric parameters on 27 delineated basins of the study area. The combined classification of Relative Tectonic Activity Index (Iat) and morphometric parameters of 27 basins categorized all the zones into four different

classes: Class 1 – Very High (<1.97; 410 km²) ; Class 2 – High (1.97 – 2.05; 275 km²) ; Class 3 – Moderate (2.05 – 2.21; 273 km²), and Class 4 – Low (>2.21; 299 km²). The basins with tectonic activities have a consistent relationship with structural disturbances, basin geometry, and field studies. The tectonically active zonation of a part of Ganga basin using geomorphic indices and morphometric parameters suggest that it has significant influence of neotectonic activities in a part of Ganga basin.

Keywords: Linear parameters; Areal parameters; Relief parameters; Geomorphic Indices; Relative Tectonic Activity Index; Ganga river basins

Introduction

The Himalaya is the youngest and tectonically active mountain chain globally subjected to active tectonism and deformational process (Valdiya 2003; Yin 2006). The evolution and modification of tectonically active regions of the mountainous terrains in the Himalaya are results of tectonic uplift, weathering and denudational processes (Valdiya 1993; Bookhagen et al. 2005; Pérez-Peña et al. 2010; Pazzaglia 2013; Joshi and Kotlia 2015). These processes of deformation affect the geomorphology, drainage pattern and landform evolution process. The tectonic disturbances

Received: 16-Aug-2018

1st Revised: 23-Jan-2019

2nd Revised: 02-Mar-2019

Accepted: 25-Apr-2019

occurring in the past can be inferred using geomorphological analysis of drainage networks (Silva et al. 2003). Hence, the study of drainage pattern will provide insights on the active tectonics that are operating in the geodynamic process of landscape development. The part of Ganga basin is exposed to slope instability, earthquakes, and active occurrences of landslides (Siddique et al. 2018). There are several landslides which are recorded along a stretch of NH – 58 is part of the study area. Neotectonics activities play a significant role in the deformational process of major disasters. Morphometric parameters and geomorphic indices act as a defining tool in determining the deformational process. These parameters also provide a valid approach to recognize, describe and evaluate modification of landforms with time (Ramírez-Herrera 1998; Azor et al. 2002; Bull 2007; Singh et al. 2008; Hamdouni et al. 2008; Pedrera et al. 2009; Dehbozorgi et al. 2010; Mahmood and Gloaguen 2012; Shukla et al. 2013; Anand et al. 2017; Cheng et al. 2018; Sharma et al. 2018). Active tectonics act as the principal aspect in the determination of recent topographic development, which considered as a combined result of erosion and denudational process (Harkins et al. 2005). The drainage pattern in the tectonically active region is susceptible to dynamic processes like folding, faulting, and tilting of the basins. These tectonic activities affect incision, asymmetry, and diversion of rivers (Cox 1994). Morphometric parameters and geomorphic indices are essential indicators to deformational processes and widely used as a reconnaissance tool for differentiation of active zones (Keller and Pinter 2002; Chen et al. 2003; Topal 2018). Evaluation of morphometric parameters and geomorphic indices on tectonically active basins assist in determining the primary reason for the anomalous behavior of basins. Hence, the distinct factors like lithology or other major discontinuity evident from the field investigations and previous studies are not the sole reason for the tectonic activities of the drainage basin. Morphometric and geomorphic indices are validated using toposheets, satellite images, aerial photographs, previous literature, and field investigations. This study helps in the assessment of active tectonics, which is very helpful in the zonation of hazards such as landslide, flood, and earthquakes. The present study is to analyze a part

of Ganga river basin (Figure 1) using morphometric parameters, geomorphic indices as assessment parameters using ASTER GDEM having a resolution of 30 m, toposheet, and satellite data (Landsat). Different type of maps such as slope map, aspect map, hill shade map, contour map, and basin maps were prepared using DEM, and toposheet were used to determine the conduct of slopes along drainage basin as shown in (Appendix 1).

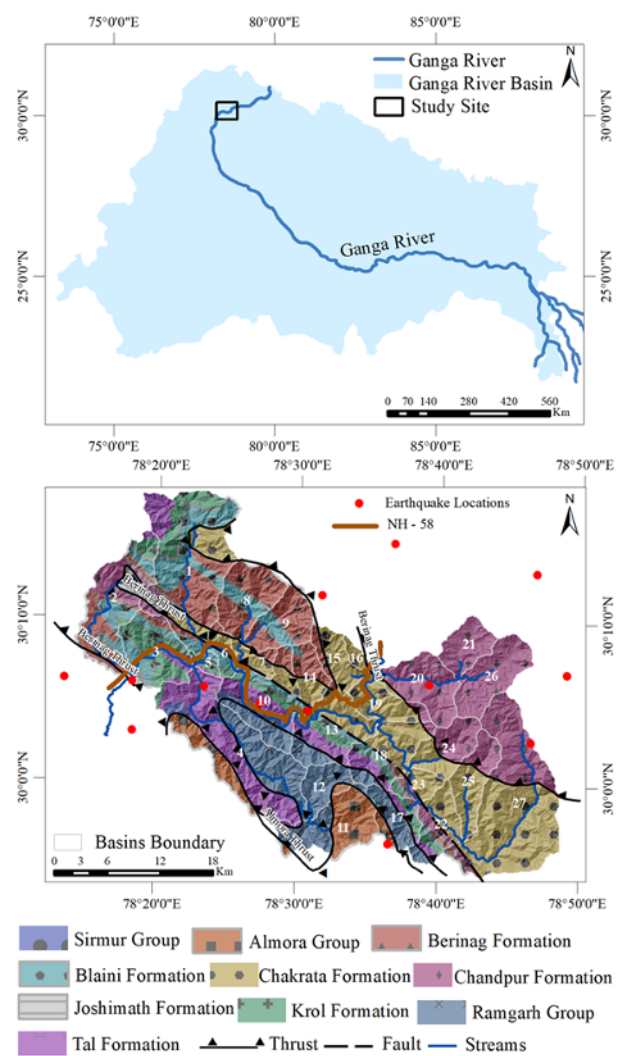


Figure 1 Regional map of Ganga river basin along with geological formations of study area (Modified after Valdiya 1980) surrounding National Highway - 58. The number represents delineated catchments in a part of Ganga River Basin.

The study area lies within the high landslide hazard zone, and seismically, it lies within the High Damage risk zone (Zone IV) of the Himalayan region (Ghosh et al. 2012). The active tectonism in

the Himalaya is the result of subduction of the Indian plate underneath the Eurasian plate. The stretch of Ganga basin lies within the tectonically active area passes through some major thrusts like Berinag thrust, Ramgarh thrust, Almora thrust, and numerous other faults. In this study, an attempt has been made to estimate the role of active tectonics in the 27 delineated basins using morphometric parameters (linear, areal and relief parameters) and geomorphic indices. These parameters and indices are correlated with seismicity and landslides prevailing in the basin. The similar approach has been used previously in different regions ([Shukla et al. 2013](#)) to determine the relative tectonic activity index (Iat) using morphometric and geomorphic Indices parameters as a decisive tool. In this study, we incorporated linear, areal and relief parameters along with geomorphic indices which have been used to determine the relative tectonic activity of the basin. The determination of tectonically active zones using morphometric parameters and geomorphic indices will precisely identify tectonically active zones. The linear parameters consist of the bifurcation ratio (R_b) and stream length ratio (L_{sr}) ([Table 1](#)). Areal parameters include drainage stream frequency (F_s), drainage density (D_d), drainage texture (D_t), elongation ratio (R_e), circularity ratio (R_c) and form factor (R_f) ([Table 2](#)). Relief parameters comprise of basin relief (R), relief ratio (R_h) and ruggedness number (H_d) ([Table 3](#)). Geomorphic indices comprise of stream length gradient index (SL), hypsometric integral (Hi), asymmetry factor (AF), basin shape (Bs), valley floor width to valley height ratio (V_f), and mountain front sinuosity index (S_{mf}) ([Table 4](#)). The categorization of these parameters into different classes such as high, moderate and low tectonically activities has been classified in previous research work. The numerical values determined for each parameter (linear, areal, relief and geomorphic indices) are categorized into three different class as Class 1, Class 2 and Class 3. Higher class (Class 1) represents higher tectonic activity while moderate class (Class 2) denotes moderate tectonic activity whereas (Class 3) represents low tectonic activity. The Iat is calculated by taking an arithmetic mean of parameters (linear, areal, and relief) and geomorphic indices to categorize into the different degree of tectonic activity.

1 Regional Setting

The study area lies within Ganga river basin along a stretch of National Highway – 58. This stretch of Ganga basin lies within the lesser Himalayan sequence. The northeastern portion of the study area mainly comprises of low-grade metamorphic rocks, metasiltstone, fine-grained greywacke along with massive shale, slates, and greywacke ([Auden 1934](#)). The southern portion consists of limestone, dolomite, and shale of Permo-Triassic age of Lesser Himalayan sequence ([Fuchs and Sinha 1975](#)). The western portion of the studied region mainly comprises of Quartzites in the inner lesser Himalayan sequences ([Valdiya 1965](#)). The uppermost region comprising of the crystalline sequence lies above Almora thrust. The lower succession consists of phyllite and quartzite. The Sirmur group comprises of Subathu formation and Singtali formation. The Sirmur group is underlaid by Tal, Krol and Blaini formation ([Valdiya 1980](#)) ([Figure 1](#)). The sequence of Tal, Krol and Blaini formation belongs to outer lesser Himalaya ([Valdiya 1976](#)). The lowermost succession comprises of Chandpur and Chakrata formations. Both the formations are separated by Berinag thrust. Chandpur formation mainly consists of low-grade metamorphics mainly phyllite while in contrast, Chakrata consists of shales, slates, and greywacke. The study area mainly comprises major thrust and faults. The major thrust includes Berinag thrust in the north, Ramgarh thrust and Almora thrust in the Southern portion. The thrust belongs to tectonically active regimes in the study area. The major fault is passing through Chakrata formation, and Blaini formation represents that basins are structurally active.

2 Material and Methods

Morphometric parameters and geomorphic indices have been extracted out on ASTER GDEM having a spatial resolution of 30 m with an accuracy of ± 10 m. The study area is a part of the Ganga River basin covering an area of 1257 km² which is subdivided into 27 sub-basins. The basin comprises of stream order ranging from third order to fifth order river basin using ([Strahler 1957](#))

Table 1 Mathematical derivation and description of linear parameters along with the classification of all the parameters in to different classes using previous literature and K - means clustering.

Linear parameters	Mathematical derivation	Description	Source	Classes	(Shukla et al. 2014)	(Sharma et al. 2018)	Classes Range adopted
Stream Order (U)	-	Interlinking of two same order streams will result in higher order streams	(Strahler 1952)	-	-	-	-
Stream number (N_u)	-	N_u = Number of stream segments of a particular order	-	-	-	-	-
Bifurcation Ratio (R_b)	N_u/N_{u+1}	N_{u+1} = Number of Stream segments of higher order	(Horton 1945)	Class 1	≥ 4	≥ 4	> 4
				Class 2	3.5-4	3.5-4	4-2.5
				Class 3	≤ 3.5	≤ 3.5	< 2.5
Stream Length Ratio (L_{ur})	L_u/L_{u-1}	L_u =Total Stream length of particular order u L_{u-1} =Total stream length of lower order	(Sreedevi et al. 2005)	Class 1	> 2.5	-	> 0.90
				Class 2	2.25-2.5	-	0.90-0.65
				Class 3	< 2.25	-	< 0.65

Table 2 Mathematical derivation and description of Areal parameters along with the classification of all the parameters into different classes using previous literature and K - means clustering.

Areal parameters	Mathematical derivation	Description	Source	Classes	(Shukla et al. 2014)	Classes Range adopted
Drainage stream frequency (F_s)	$\sum N_u/A$	$\sum N_u$ = Total number of segments of all order in a basin A= Area of the Basin	(Horton 1945)	Class 1	> 0.85	> 7.30
				Class 2	0.80-0.85	7.30-5.90
				Class 3	< 0.80	< 5.90
Drainage density (D_d)	$\sum L_t/A$	$\sum L_t$ = Total length of each stream order of the basin A= Area of the Basin	(Horton 1945)	Class 1	> 0.95	≥ 2.10
				Class 2	0.90-0.95	2.09-2.00
				Class 3	< 0.90	< 2.00
Drainage texture (D_t)	$\sum N_u/P$	Perimeter (P) of the basin	(Horton 1945)	Class 1	≥ 0.8	> 10
				Class 2	0.7-0.8	10- 5
				Class 3	≤ 0.7	< 5
Elongation ratio (R_e)	$1.128\sqrt{A/L_b}$	A= Area of the Basin L_b = Length of the Basin	(Schumm 1956)	Class 1	< 0.6	< 0.85
				Class 2	0.6-0.7	0.85 – 1.25
				Class 3	> 0.7	> 1.25
Circularity ratio (R_c)	$4\pi A/P^2$	A= Area of the Basin Π = 3.14 ; P = Perimeter of the Basin	(Horton 1945)	Class 1	< 0.4	< 0.35
				Class 2	0.4-0.5	0.35-0.40
				Class 3	> 0.5	> 0.40
Form Factor (R_f)	A/Lb^2	A= Area of the Basin Lb^2 = Square of Basin length	(Horton 1945)	Class 1	< 0.3	< 0.55
				Class 2	0.3-0.4	0.55-1.50
				Class 3	> 0.4	> 1.50

method of stream ordering. The linear, areal and relief parameters are evaluated using different parameters of DEM, eg. Stream order, stream number, stream length, area, perimeter, and basin elevations are measured using ARC GIS 10.6. The linear, Areal and relief parameters are discussed in detail in (Appendix 2). The Geomorphic Indices

calculated on six parameters for evaluation of 27 basins of the study area. The detailed description of geomorphic indices parameters are as follows:

Asymmetry factor (AF) is a significant tool in determining the tectonic tilting of the basin. The tectonic disturbance results in shifting of the main channel from the midline in the direction of tilting

Table 3 Mathematical derivation and description of Relief parameters along with the classification of all the parameters into different classes using previous literature and K - means clustering.

Relief parameters	Mathematical derivation	Description	Source	Classes	(Shukla et al. 2014)	Classes Range adopted
Basin Relief (R)	$Z - z$	$Z = \text{Elevation of highest point of the basin}$ $z = \text{Elevation at mouth}$	(Strahler 1952)	Class 1	>1.60	>1.60
				Class 2		1.60-1.30
				Class 3		<1.30
Relief Ratio (R_h)	R/L_b	$R = \text{Basin Relief}$ $L_b = \text{length of the basin}$	(Schumm 1956)	Class 1	>0.1	>0.29
				Class 2	0.05-0.1	0.28-0.17
				Class 3	<0.05	<0.17
Ruggedness number (Hd)	$R \times D_d$	$R = \text{Basin Relief}$ $D_d = \text{Drainage Density of the Basin}$	(Schumm 1956)	Class 1	>600	>3.25
				Class 2	400-600	3.24-2.66
				Class 3	<400	<2.66

(Figure 2a and 2b). The AF can be applied at the drainage basin scale, as it can be applied over a larger area (Hare and Gardner 1985). It is defined as:

$$AF = (A_r/A_t) \times 100 \quad (1)$$

where A_r (km²) is the area of the basin to the right of the main channel facing downstream and A_t (km²) expressed as the total area of the basin (Figure 2c) and Eq.(1).

Valley floor width to valley height ratio (Bull and McFadden 1977) has been defined to discriminate between U shaped valleys and V-shaped valleys. It is responsive to tectonic uplift and defined as the ratio of valley floor width to valley height (V_F) as below.

$$V_F = \frac{2V_{fw}}{(E_{ld}-E_{sc})+(E_{rd}-E_{sc})} \quad (2)$$

V_{fw} is the width of the valley floor whereas E_{ld} and E_{rd} represent the elevation of the left and right valley divide facing downstream while E_{sc} represents the elevation of the valley floor (Figure 2d and 2e) and Eq.(2).

Hypsometric curves and Hypsometric Integrals are essential parameters of drainage basin development regarding its erosional and depositional activities (Figure 2f, 2g and 2h). Hypsometric curves are an estimation of basin development regarding depositional and erosional sequences (Hurtrez et al. 1999; Singh et al. 2008).

The hypsometric integral has been calculated using (Pike and Wilson 1971) and Eq.(3)

$$Hi = \frac{(Elevation_{avg} - Elevation_{min})}{(Elevation_{max} - Elevation_{min})} \quad (3)$$

where Hi is the hypsometric integral, $Elevation_{avg}$ is the average elevation, $Elevation_{min}$ and $Elevation_{max}$ is the lowest and highest elevation of the basin,

respectively (Figure 2i). The index has been calculated using elevation at different points of the basin (Mayer 1990; Keller and Pinter 2002). Higher index values of Hi might result from the recent incision of initial landforms formed by deposition.

The SL index works on a quantitative approach which is related to erosional and depositional processes. The stream length gradient index (Hack 1973) defined as

$$\text{Stream Length Gradient Index (SL Index)} = (\Delta H / \Delta L_r) L_t \quad (4)$$

where ΔH defined as the difference in altitude and ΔL_r is the length of the reach and L_t is the horizontal length from watershed divide to the midpoint of the reach. The SL index is calculated along the main river channel and its tributaries using Eq.(4) and (Figure 2j and 2k).

The shape of the basins in tectonically active mountain ranges is much more elongated in shape which attains circular shape with evolution (Bull and McFadden 1977). It is defined as the ratio of

$$\text{Basin shape} = \frac{B_l}{B_w} \quad (5)$$

B_l is the measured length from headwater to the point on the mouth of the basin, whereas B_w is the measured width at the widest point on the basin (Ramírez-Herrera 1998) (Figure 2l) and Eq.(5).

The mountain front sinuosity index has been defined by (Bull and McFadden 1977) and (Bull 1978) as

$$S_{mf} = \frac{L_{mf}}{L_s} \quad (6)$$

where L_{mf} has been defined as the planimetric length of a mountain front while L_s is the length of a mountain front measured along a straight line

Table 4 Mathematical derivation and description of Geomorphic Indices along with the classification of all the parameters in to different classes using previous literature and K means clustering.

Geomorphic indices	Mathematical derivation	Description	Source	Classes	Mahmood and Gloaguen 2012	Sharma et al. 2018	Deboozorgi et al. 2010	Classes Range adopted
Asymmetry factor (AF) $= (A_r/A_t) \times 100$	$A_r = \text{Area of the Basin to the right of main channel facing downstream}$ $A_t = \text{Total area of the basin}$ $V_{fw} = \text{Valley floor width}$ $E_{ld} = \text{Elevation of left valley divide ; } E_{rd} = \text{Elevation of right valley divide ; } E_{sc} = \text{Elevation of valley floor}$ $(E_{ld} + E_{rd} - 2E_{sc}) / (2V_{fw})$	(Hare and Gardner 1985)	Class 1 Class 2 Class 3	> 5.91 2.95 - ≤ 5.91 ≤ 2.95	> 15 5-15 < 5	-	> 18 18-7 < 7	
Valley floor width to height ratio (V_f)		(Bull and McFadden 1977)	Class 1 Class 2 Class 3	0.02-0.44 0.45-1.0 1.01-3.25	< 0.5 0.5-1.0 ≥ 1.0	≤ 0.5 0.5-1.0 ≥ 1.0	< 0.25 0.25-0.40 ≥ 0.40	
Hypsometric Integral (Hi)	$\frac{(E_{avg} - E_{min})}{(E_{max} - E_{min})}$	(Strahler 1952)	Class 1 Class 2 Class 3	0.51-0.78 0.37-0.50 < 0.37	> 0.47 0.46-0.47 < 0.46	> 0.5 0.4-0.5 < 0.4	≥ 0.40 0.39-0.30 < 0.30	
Stream length Gradient Index (SL Index)	$(\Delta H / \Delta L_r) L_t$	$\Delta H = \text{Change in Altitude}$ $\Delta L_r = \text{Length of the reach}$ $L_t = \text{Horizontal length from the watershed divide to midpoint of the reach.}$	(Hack 1973)	Class 1 Class 2 Class 3	≥ 1076-750 749-365 < 365	≥ 2000 2000-500 < 500	≥ 500 500-300 < 300	≥ 400 400-200 < 200
Basin shape (B_s)	B_l/B_w	$B_l = \text{Basin length from Head point to mouth}$ $B_w = \text{Width of the Basin}$	(Ramírez-Herrera 1998)	Class 1 Class 2 Class 3	1.77-3.22 1.21-1.76 1.11-1.20	> 1.76 1.11-1.76 < 1.11	≥ 4 3≤-<4 ≤ 3	> 2.30 2.30-1.120 < 1.20
Mountain Front sinuosity index (S_{mf})	L_{mf}/L_s	$L_{mf} = \text{Planimetric length of mountain front along the mountain piedmont junction ;}$ $L_s = \text{length of the mountain front measure along straight line}$	(Bull 2007)	Class 1 Class 2 Class 3	1.00-1.09 1.1-1.16 > 1.16	< 1.2 1.2-1.5 > 1.5	< 1.1 1.1-1.5 ≥ 1.5	< 1.16 1.16-1.30 ≥ 1.30

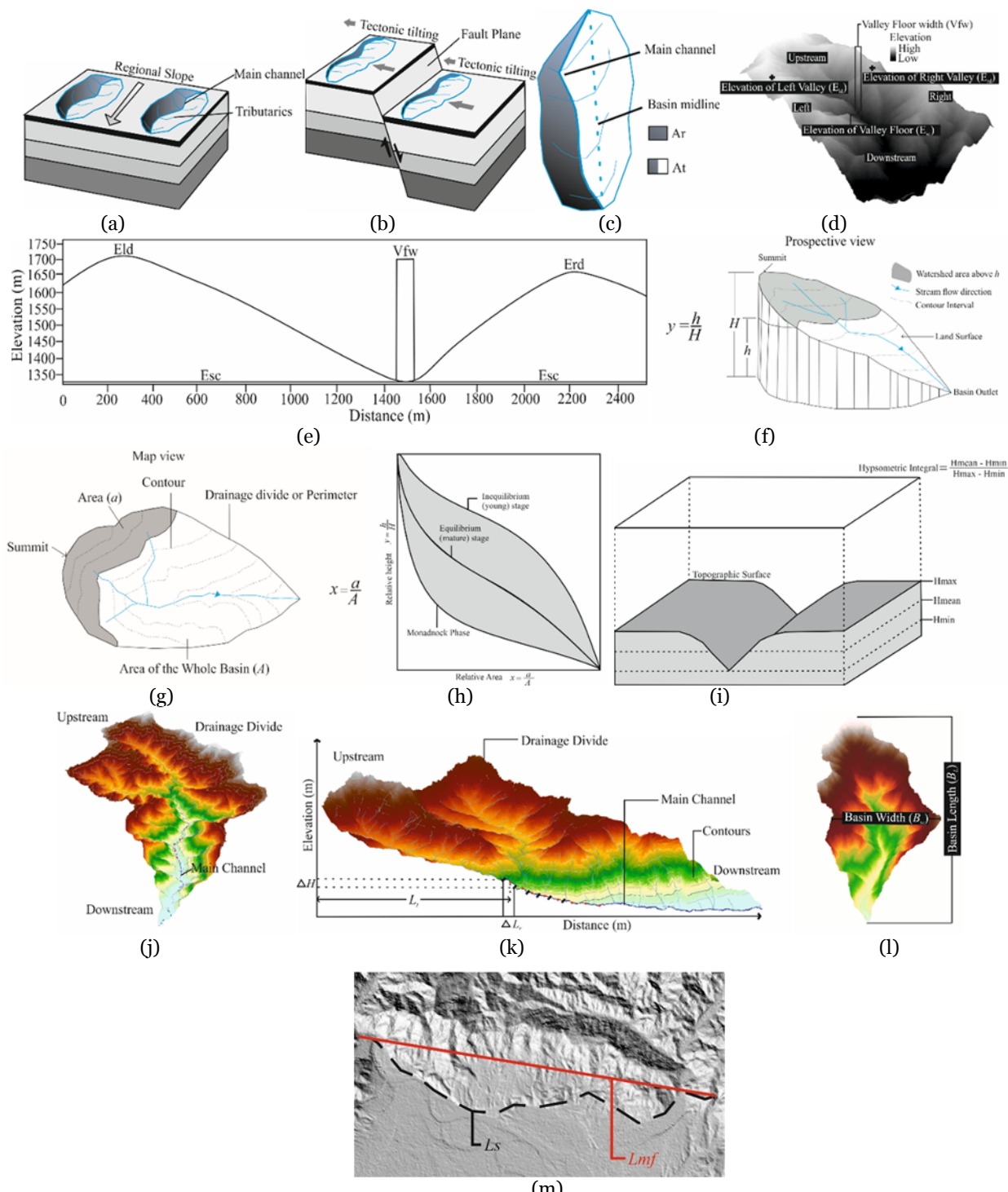


Figure 2 Methodological description of Geomorphic Indices parameters (a) Normal flow conditions of a river basin; (b) Shifting of the main river channel due to a normal fault condition; (c) Asymmetry factor parameters representing the area of the basin to the right of the main channel (A_r) facing downstream whereas (A_t) represents the total area of the basin (modified after Mahmood and Gloaguen 2012 and Keller and Pinter 2002); (d) Three dimensional perspective view of valley representing parameters of valley floor width to valley height ratio; (e) Two dimensional perspective view of parameters of valley floor width to valley height ratio; (f) Geomorphic cycle of development as prospective view; (g) Geomorphic cycle of development as map view; (h) Hypsometric curves representing Inequilibrium, Mature and Monadnock stage of the basin; (i) Topographic surface representing parameters of the Hypsometric integral (modified after Strahler 1952); (j) Three dimension perspective view representing drainage divide and contours of the basin; (k) Stream Length gradient Index parameters (modified after Gaidzik and Ramírez-Herrera 2017); (l) Perspective view of Basin Shape Index representing Basin Length (B_L) and Basin Width (B_w); (m) Parameters of Mountain front sinuosity index.

(Figure 2m) and Eq.(6). The values determined for each parameter are categorized into different classes based on previous literature and K – means clustering. The classes of each basin are averaged to determine the basins with higher, moderate and low tectonic activities. The earthquake data downloaded from (USGS 2018) and the International Seismological Centre (ISC 2016) from 1901 - 2018. The landslide susceptibility mapping is performed by recording the number of landslides in the field and analysis of the angle of failure of slope facets (GSI 2016). The computed parameters of the earthquake, landslide susceptibility mapping, and field investigations were integrated to validate the significance of Iat in the study area.

3 Results

3.1 Linear parameters

The linear parameters have been evaluated using stream order (U), stream number (N_u), stream length ratio (L_{ur}) and bifurcation ratio (R_b). The objective of this analysis is to define the evolution of the basin as one-dimensional characteristics using bifurcation ratio and stream length ratio as parameters for evaluation. The main river channel (Ganga River) belongs to stream order of the seventh order. The higher values of R_b represent youth stage while lower values represent a mature stage of basin development (Manu and Anirudhan 2008). The values of the bifurcation ratio in the study area range from 1.60 to 8.78. Stream length ratio (L_{ur}) defined as the ratio of mean stream length of the higher order to the lower order. Slope and topographic conditions have a profound role in the variation of L_{ur} in successive streams. It has a significant role in surface flow discharge and erosional stage of the basin (Sreedevi et al. 2005). The values of L_{ur} varies from 0.47 to 1.25 in the study area. The values calculated for each linear parameter characterized into three classes of high (Class 1) moderate (Class 2) and low (Class 3) tectonically active zones using previous literature and K – means Clustering (Table 1). The values determined for each basin averaged and categorized into three classes as Class 1, Class 2 and Class 3 (Figure 3a) to determine the

tectonically active basin.

3.2 Areal parameters

The areal parameters include drainage density (D_d), drainage (Stream) frequency (F_s), drainage texture (D_t), elongation ratio (R_e), circularity ratio (R_c) and form factor (R_f). These parameters are evaluated to interpret the erosional activity of the basin. The D_d of the basin influenced by geological setup, soil properties, vegetation and intensity of rainfall (Horton 1945). The values of drainage density in the study area vary between 1.75 and 2.24. Higher values of D_d , F_s , and D_t in the drainage basins are results of impermeable lithological conditions, low infiltration capacity and high relief conditions (Ozdemir and Bird 2009; Shukla et al. 2013). The lower values of D_d , F_s , and D_t are indicative of permeable lithology, high infiltration capacity and lower relief of basins. The basins in the study area consist of both higher and lower values of drainage density, drainage stream frequency, and drainage texture respectively. The shape of the drainage basin is characterized by elongation ratio, circularity ratio, and form factor. The lower value of the elongation ratio represents elongated basins while the higher value represents circular basins (Strahler 1964). In the study area, the calculated value of the elongation ratio varies from 0.50 to 1.75. The basins with lower values of R_e are susceptible to the erosional environment of the drainage basin (Sreedevi et al. 2009). The circularity ratio depends on the geological setup, slope and land cover (Sreedevi et al. 2009) of the basins. The values of circularity ratio vary between 0.24 and 0.46. The higher values of R_c indicates basins with circular basins which tends to attain an elongated shape with time. The form factor varies from 0.20 to 2.41 for the study area. The lower values of form factor indicate elongated basins which suggest that basins are structurally and tectonically controlled. The values of areal parameters are classified into various classes from High to low tectonic activity from previous literature and K- means clustering (Figure 3b and Table 2).

3.3 Relief parameters

Basin relief, relief ratio, and ruggedness number are interpreted parameters of the study

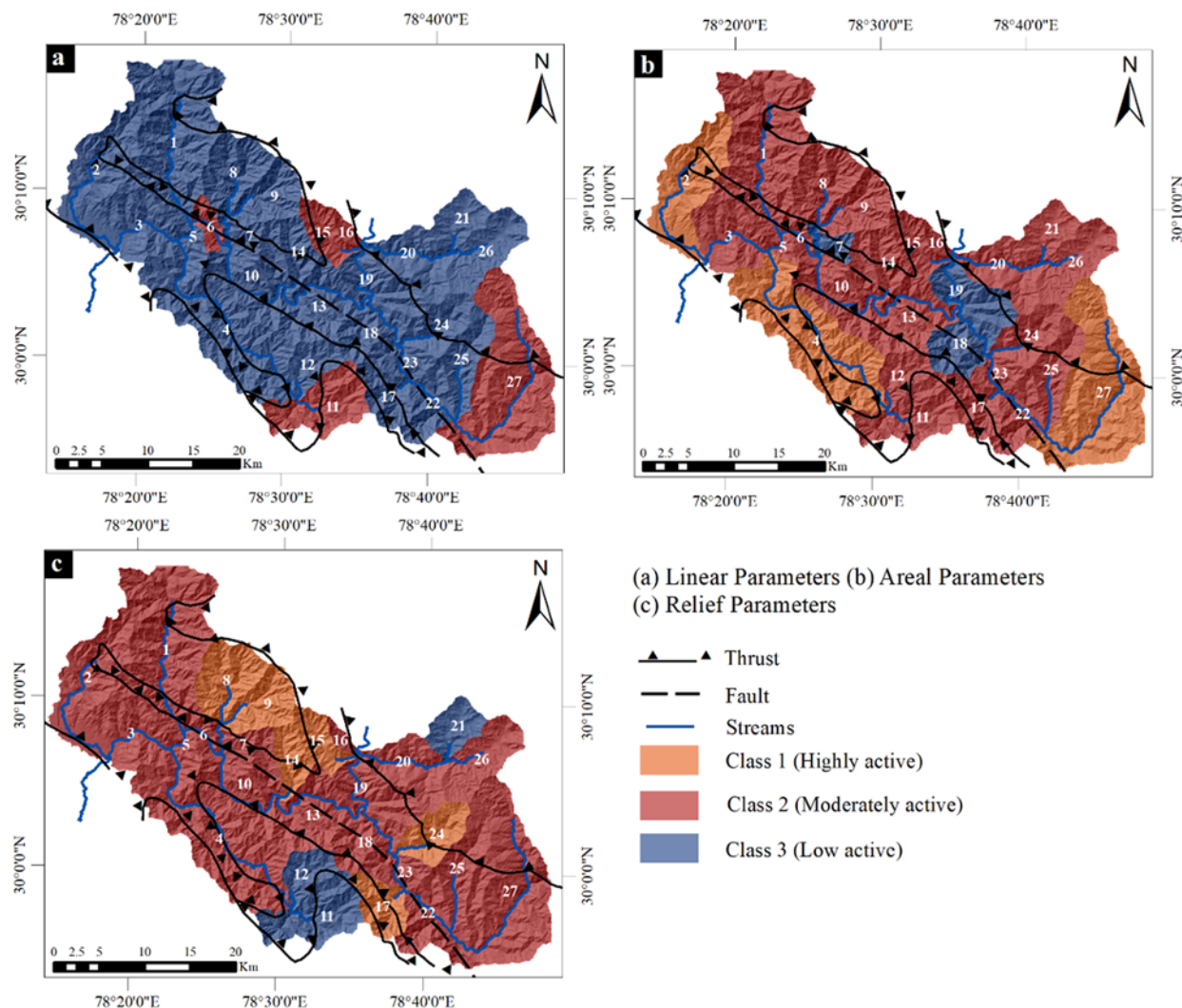


Figure 3 Cumulative representation of (a) Linear parameters (R_b and L_{ur}), (b) Areal parameters (F_s , D_d , D_l , R_e , R_c , R_f) and (c) Relief Parameters (R , R_h , and H_d) on 27 basins of the study area.

area to evaluate the denudational characteristics of the basin (Table 3). The basin relief is characterized by the difference in the highest and lowest points of the basin. The relief ratio defined as the ratio of basin relief to the length of the basin. The values of relief ratio vary from 0.06 to 0.44. The lower value of relief ratio is a characteristic feature of less resistant rocks and vice-versa. Ruggedness number (H_d) represents a range of values from 1.82 to 4. The lower value of H_d in the drainage basin implies that the area is less prone to soil erosion and disposed to intrinsic structural complexity. The class interval for each parameter (linear, areal and relief) has been divided into three classes, and the class number assigned to each parameter of the 27 Basins (Table 3). The average

of all the three relief parameters was computed to determine the basin with higher to lower tectonic activity (Figure 3c).

3.4 Results of geomorphic indices

Geomorphic Indices were determined to analyze topography, drainage network and the role of relative active tectonic in the deformational process (Hamdouni et al. 2008; Topal et al. 2016). The Geomorphic Indices determined for all the 27 basins which are part of Ganga River Basin (Table 4). The parameters of geomorphic indices were averaged along with linear, areal and relief parameters to determine the lat.

Asymmetry factor is sensitive to change in inclination perpendicular to the direction of the stream (Mahmood and Gloaguen 2012). The value of AF close to 50, suggest no or slight tilting perpendicular to the stream flow. The value of AF significantly higher or lesser than 50, shows more tilting and represents the influence of active tectonics in the basin (Alipoor et al. 2011). Displacement of faults has resulted in steeper landforms in the tectonically active regimes of the basins. Structurally controlled basins have an inclination of the valley in down dip direction which results in the asymmetric valley (Hamdouni et al. 2008). The asymmetric factor is calculated for 27 river basins to evaluate the tectonic tilting of the basins. The calculation of the asymmetry factor regarding Iat absolute value calculated using the difference between observed value and neutral value (50). The arrow is indicating asymmetry direction of the basins as shown in (Figure 4a). The $|AF-50|$ is evaluated and categorized into three classes namely: Class 1 (>18), Class 2 ($18-7$) and Class 3 (<7). Basin 13 with the highest AF value represents strongly asymmetrical basin while Basin 12 with the lowest value represent gently asymmetric basin. Class 1 indicates strongly asymmetrical basin while Class 2 and Class 3

represent moderately asymmetric basin and gently asymmetric basin. The values of an asymmetric factor for Class 1 range from 32.26 to 22.34, for Class 2 range from 18.21 to 8.99 and for Class 3 range from 7.71 to 0.04 (Figure 4b and Table 5).

Valley floor width to valley height ratio (V_f) helps in determining tectonic uplift in the narrow and U-shaped valley floor (Bull and McFadden 1977; Bull 1978). Higher values are representatives of U shaped valley while V-shaped valleys depict lower values. Active tectonic uplifts along with incision are associated with narrow shaped valley although wide valleys have attainment of a base level of erosion. The parameter is interdependent upon basin area, geometry, stream discharge, and lithological setting which acts as a proxy for active tectonics. The values of the valley floor are calculated on 282 locations covering 27 studied basins, and major thrusts, faults and rivers passing through the basins have been marked in (Figure 5a). Basin 2 consists of the highest value while basin 17 consists of the lowest value of V_f . It has been classified into three classes Class 1 (<0.25), Class 2 ($0.25 - 0.40$) and Class 3 (>0.40), and most of the valley are V-shaped valleys which are exposed active tectonic process (Figure 5b).

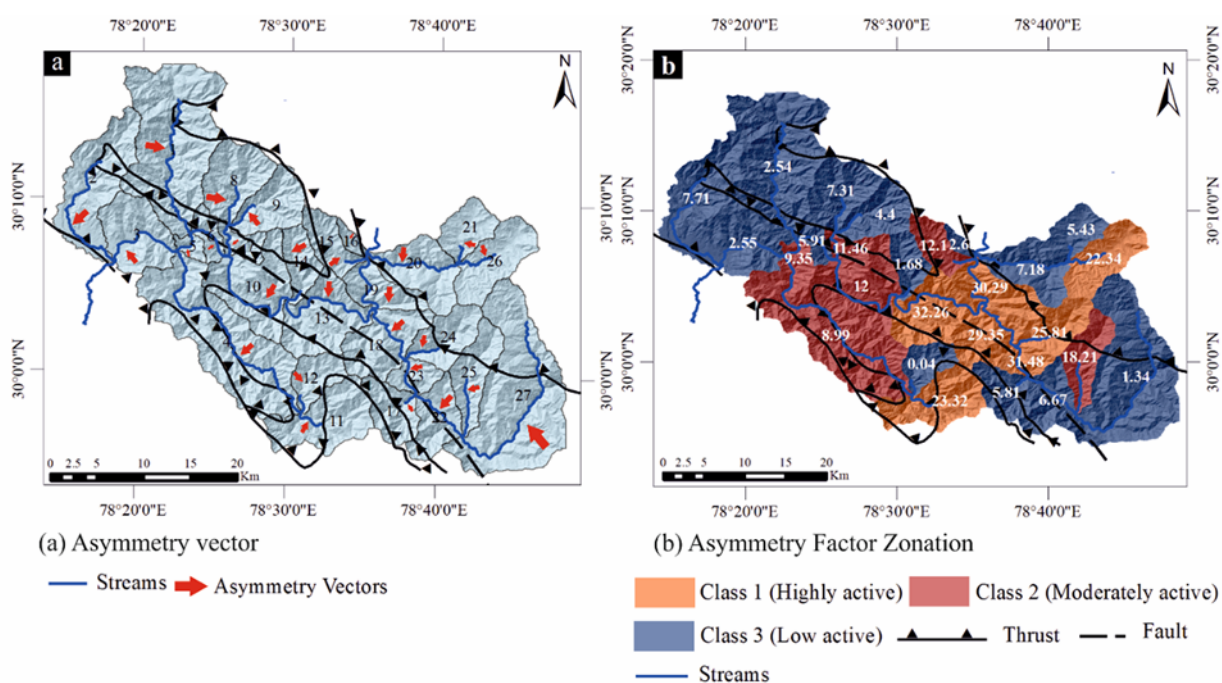


Figure 4 Directions and classification of tectonic tilting of the basins (a) Asymmetry vector representing tectonic tilting of the basins (b) Asymmetry factor map representing three classes of strongly asymmetric basin (Class 1), moderately asymmetric basin (Class 2) and less asymmetric basin (Class 3).

Hypsometric integral estimates the volume of the basin that has not been eroded (Hamdouni et al. 2008). Values on the higher side of Hi are indicative of the development of recent landforms resulted from active tectonics (Hamdouni et al. 2008). The convex, S-shaped and concave hypsometric curves are determined for each basin as shown in (Appendix 3, B1-B27). The geomorphic cycle of the basin is representative of the young, mature and old stage of basin development (Smith et al. 2009). The hypsometric curves of all the basins are cumulatively plotted to represent a young, mature and old stage of the basins (Figure 6a). The characteristic shapes of hypsometric curves along with Hi values work as defining a parameter for calculation of Iat (Hamdouni et al. 2008; Mahmood and Gloaguen 2012; Cheng et al. 2018). The Hi values of 27 basins are computed using Eq.(3), and its values vary between 0.12 (Basin 19) to 0.51 (Basin 21). The highest value of Hi is calculated for basin 21 while the lowest value has been calculated for basin 19. The computed values are divided into three different classes as Class 1 (≥ 0.40) represents convex hypsometric curves, Class 2 (0.39-0.30) depicts concave – convex hypsometric curves and Class 3 (< 0.30) are representatives of concave hypsometric curves. The

Table 5 Calculated values of Geomorphic indices parameters of 27 Basins of the study area.

Basin Index	Geomorphic Indices					
	SL	Hi	AF	Bs	V _f	S _{mf}
1	342	0.23	2.54	1.92	0.36	1.10
2	300	0.2	7.71	3.15	0.72	1.74
3	189	0.22	2.55	0.69	0.22	1.18
4	198	0.24	8.99	3.22	0.18	1.29
5	64	0.18	9.35	0.62	0.17	1.28
6	119	0.18	5.91	0.44	0.23	1.10
7	366	0.38	11.46	0.41	0.21	1.20
8	384	0.27	7.31	1.27	0.14	1.18
9	357	0.27	4.40	1.47	0.14	1.09
10	382	0.34	12.00	1.03	0.22	1.13
11	287	0.28	23.32	0.47	0.20	1.50
12	310	0.35	0.04	1.34	0.15	1.10
13	293	0.25	32.26	0.89	0.25	1.45
14	448	0.33	1.68	2.35	0.15	1.09
15	516	0.33	12.10	2.72	0.22	1.17
16	570	0.42	2.68	3.03	0.12	1.08
17	374	0.34	5.81	0.69	0.10	1.15
18	337	0.31	29.35	0.53	0.11	1.19
19	69	0.12	30.29	0.37	0.20	1.28
20	390	0.31	7.18	1.72	0.21	1.08
21	316	0.51	5.43	1.57	0.39	1.12
22	366	0.25	6.67	0.64	0.34	1.11
23	368	0.35	31.48	1.04	0.31	1.74
24	478	0.36	25.81	2.08	0.15	1.13
25	454	0.35	18.21	3.18	0.14	1.08
26	385	0.4	22.34	0.41	0.30	1.13
27	392	0.28	1.34	2.55	0.19	1.26

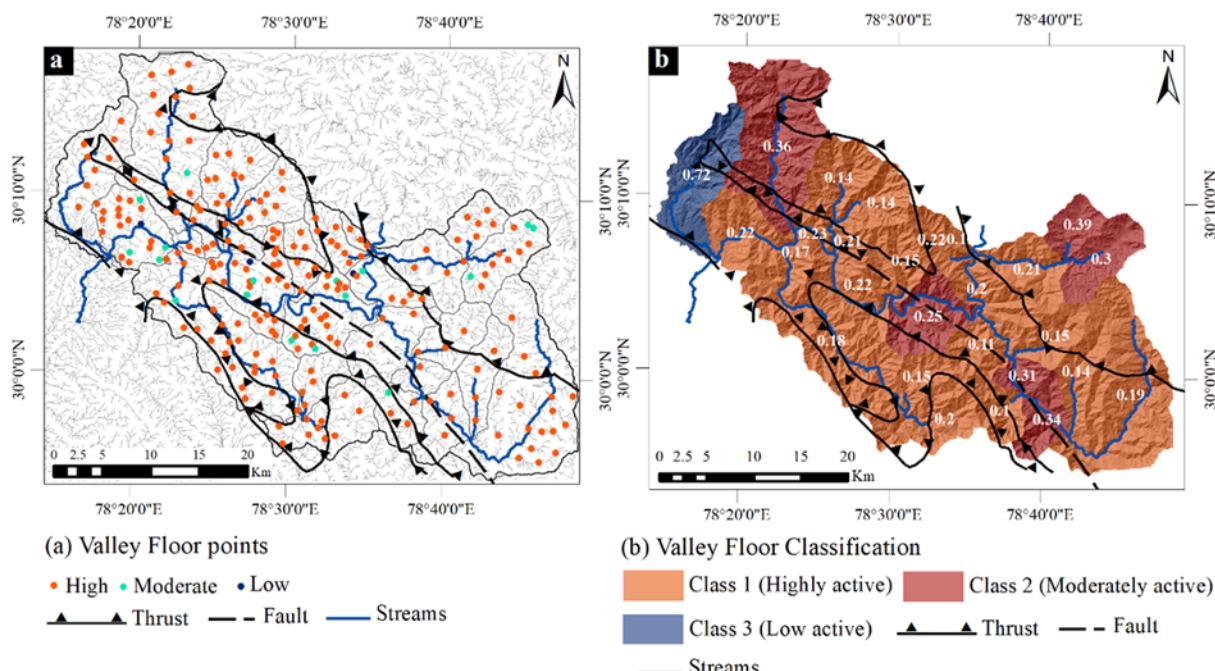


Figure 5 Locations and classification of valley floor width to valley height ratio (V_f) on 27 studied basins of Ganga River (a) V_f points of 282 locations and their categorization into High (Class 1), Moderate (Class 2) and Low (Class 3) of tectonic activity. (b) Classification of V_f into various classes.

range of class 1 to class 3 is representative of young, mature and monadnock stage of drainage basin development (Figure 6b).

The values of *SL* index are dependent on the change in channel slope, rock resistance and topography (Keller and Pinter 1996). It works on river channel morphology along with tectonically derived features (Alipoor et al. 2011). The flow of river over terrains of the variable rock strength and soil tend to reach an equilibrium which can be determined with the help of *SL* Index. The

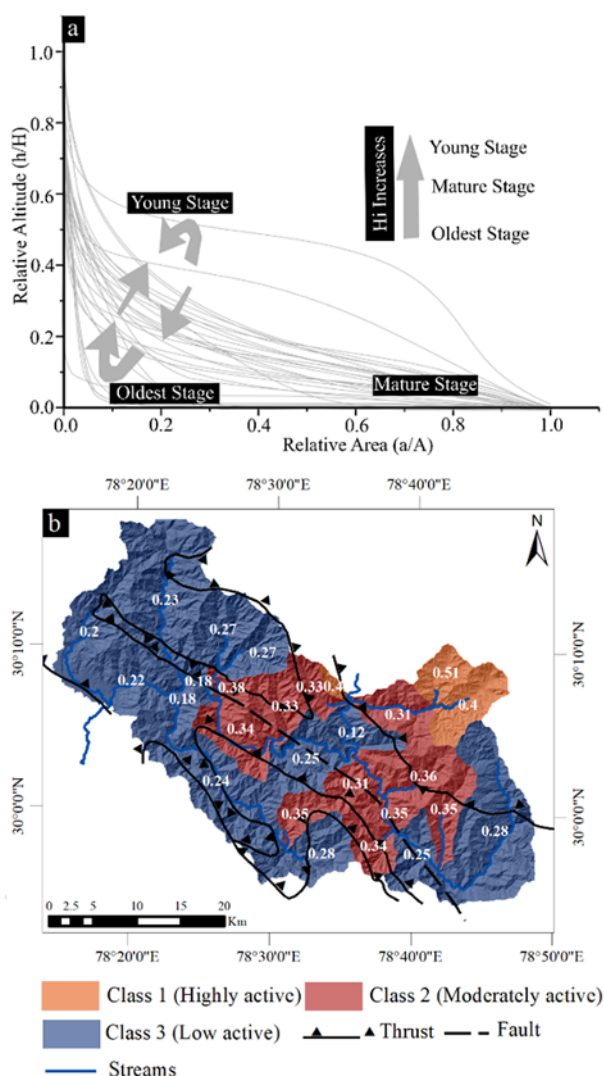


Figure 6 Cumulative representation of Hypsometric curves and Hypsometric Integral classes of 27 basins of the study area (a) Hypsometric curves representing young, mature, and old stage while hypsometric integral values increases in the youngest stage of landform and vice versa. (b) Classification of Hypsometric Integral values into various classes of tectonic activities.

deviation in the river profile might result from tectonic, lithological and environmental parameters (Hack 1973; Bull 2007). The *SL* values were plotted on the rock strength map to evaluate the impact of variable rock strength on *SL* Index. The major thrust like Ramgarh thrust, Berinag thrust, Almora thrust are passing through the actual river profile have higher *SL* index values. The rock strength map is prepared based on the lithological, structural and tectonic parameters. Rock strength map with variable *SL* index values is used to determine the role of tectonic activity (Figure 7a). The soft rock terrain comprises of high *SL* values which depict that area is under the influence of recent tectonic activities. However, higher *SL* values determine that tributaries are passing through strike-slip faults (Keller and Pinter, 2002). The highest value of *SL* index is computed for (Basin 5) while the lowest value is computed for (Basin 16). The *SL* values categorized into three classes as Class 1 (>400), Class 2 (400–200) and Class 3 (<200) using previous literature and K – means clustering (Figure 7b and Table 4). The *SL* values are plotted for each basin on the streams to determine the stream channel with high or low structural controls as shown in (Appendix 4, B1–B27).

The higher values of basin shape indicate elongated basins which estimate higher tectonic activity. The basins with lower values tend to have a circular shape and denote lower tectonic activity. The mountain fronts of tectonically active regimes have much narrower widths where streams have been directed primarily to the downcutting direction. In contrast, the areas lacking continuing rapid uplift are permissible for the widening of the basin upstream of mountain front (Ramírez-Herrera 1998). Basin 4 represents an elongated basin with higher tectonic activity while Basin 19 represents the lowest value of *Bs*. The *Bs* values classified into three classes as Class 1 (>2.30), Class 2 (2.30 – 1.20) and Class 3 (<1.20). The calculated values of the basin shape range from 0.37 (Basin 19) to 3.22 (Basin 4). The basin belongs to Class 1, and Class 2 are tectonically active basins and are elongated in shape (Figure 8a).

The S_{mf} has been calculated to evaluate the relative tectonic activity along the mountain front (Keller and Pinter 2002). Inactive mountain fronts yield straight front while active mountain fronts

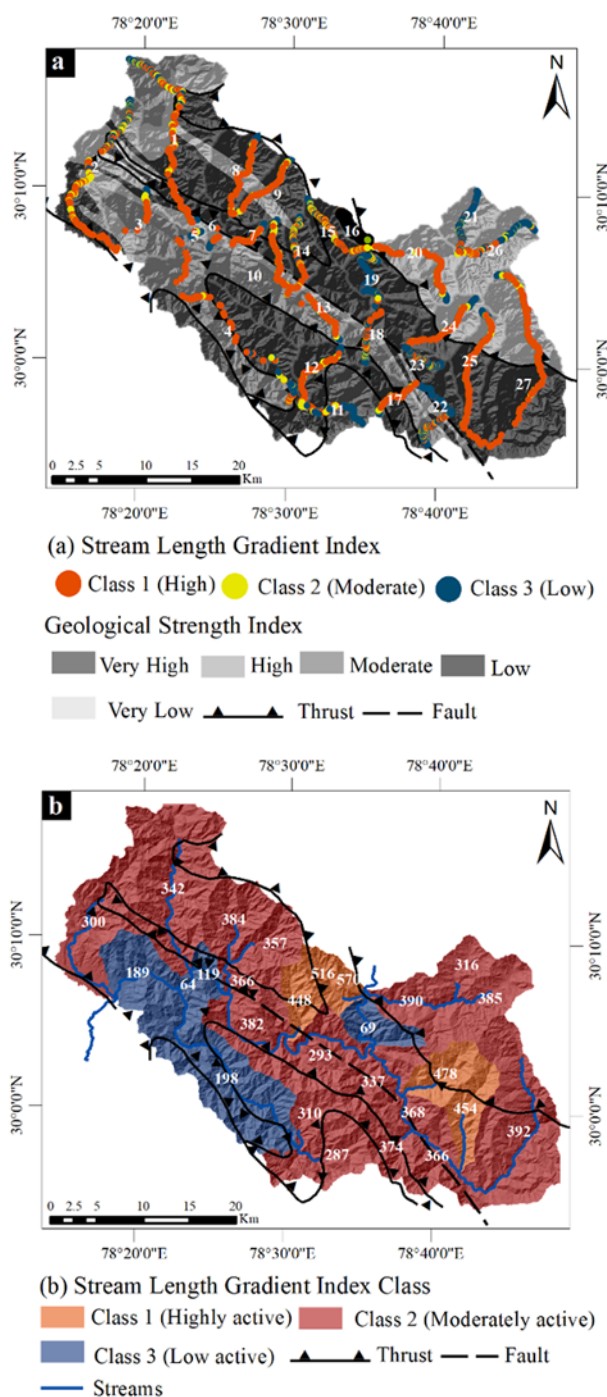


Figure 7 Correlation of Stream Length gradient index values with geological strength map and distribution of stream length gradient index (SL) classes on the studied basins (a) Distribution of SL index values on geological strength level map of the study area (b) SL gradient Index classes of different basins.

erosional processes generate sinuous fronts with higher S_{mf} values (Bull 2007). (Keller 1986) has identified that lower S_{mf} values (<1.4) are indicative of tectonically active fronts while higher S_{mf} values

(>3) represent inactive fronts. The values of S_{mf} have been calculated on 34 mountain fronts on DEM. The basin 16 with the lowest value represents tectonically active front in comparison with Basin 23 which consist of the highest value. The values of the mountain front sinuosity index have also been categorized into three classes as Class 1 (<1.16), Class 2 (1.16 – 1.30) and Class 3 (>1.30). The value of S_{mf} ranges from 1.08 to 1.74 (Figure 8b).

4 Discussion

The main goal of this study is to analyze, evaluate and quantify the role of active tectonics in the lesser Himalayan zone. The assessment of relative tectonic activity in the past has been done using a limited number of geomorphic indices (Bull and McFadden 1977; Azor et al. 2002; El Hamdouni et al. 2008; Dehbozorgi et al. 2010). The investigation of the present study is to decipher active tectonism in 1257 km² area on 27 basins using linear, areal and relief parameters with geomorphic indices.

4.1 Linear, areal and relief parameters

Linear, areal and relief parameters are calculated on 13 parameters along a stretch of NH – 58 on the delineated basins. (Strahler 1952) method of stream ordering has been used for drainage basin delineation. Stream order of 27 basins of the study area varies from third order river basins to fifth order river basins. As the number of streams is higher in first order which gradually decreases as stream order increases. The lower order streams are higher in number in the highly dissected drainage basins of the study area. Basins with higher R_b are passing through Berinag thrust, Ramgarh thrust, and Almora thrust. All the calculated parameters are categorized into different classes to determine the field with active tectonics. The two parameters, i.e., bifurcation ratio and stream length ratio are divided into three classes. Majority of the basins come under moderate active tectonics (247 km²) and low active tectonics (1010 km²) zone (Figure 3a). The areal parameters have been evaluated, and the basins come under high (357 km²) and moderately active (811 km²) zone

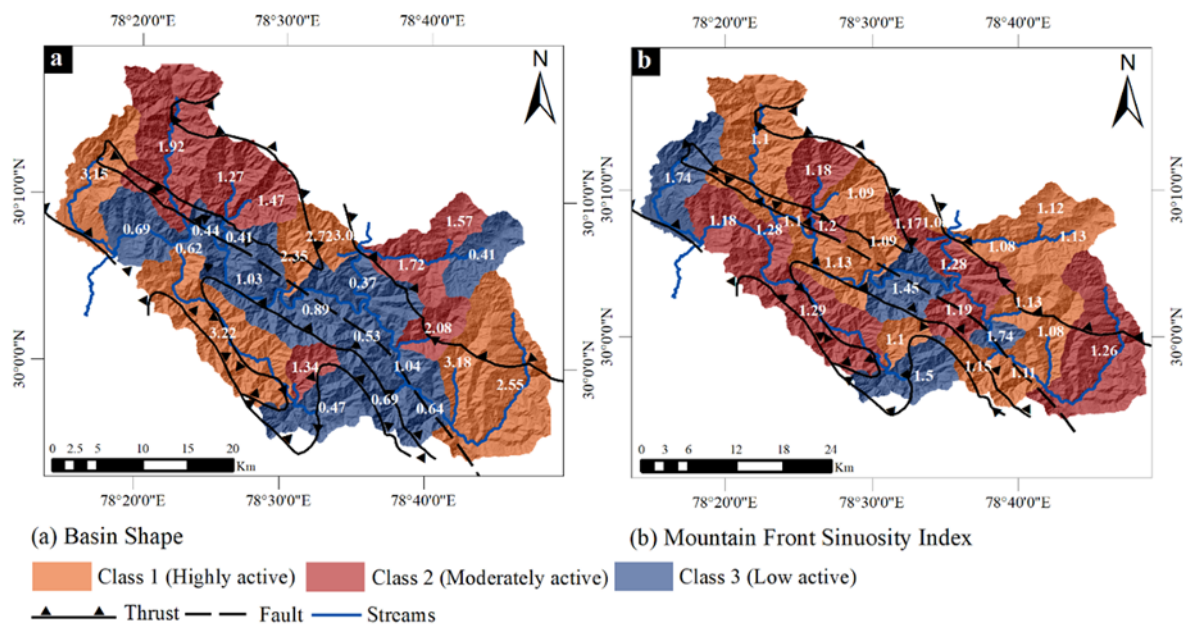


Figure 8 Distribution of Basin shape and Mountain Front Sinuosity Index classes in a part of the Ganga River basin
(a) Classification of Basin shape. (b) Classification of Mountain front sinuosity Index.

and low active zone (89 km^2) (Figure 3b). The active tectonics of relief parameters were categorized into three different parameters, i.e., relative relief, relief ratio, and ruggedness number. The majority area lies within a moderately active zone (Figure 3c). Tectonically active zones of relief parameters are passing through Berinag thrust.

4.2 Geomorphic Indices as a tool for Relative Tectonic Activity Index

4.2.1 Asymmetry factor

The substantial shifting of drainage basin results from tectonic activities. In this study, basins belong to Class 1 (>18) correspond to the NE portion as these form a zone which corresponds to a tectonic tilting of the basin. High tectonically activity zone covers an area of 284 km^2 which is passing through major faults and thrusts. The study area comprises 22 % (Class 1), 22 % (Class 2) and 56 % (Class 3) (Figure 4b). The outcome obtained from asymmetry factor analysis results from large-scale tilting phenomena which might be due to the passing of Berinag, Ramgarh and Almora thrust and faults passing through the basins. The basin which corresponds to tilting activities has a profound correlation with seismic activities and active landslides.

4.2.2 Valley floor width to valley height ratio

The low values of the valley floor width to valley height ratio correspond to V-shaped valley while higher values of V_f corresponds to U shaped valley. The V_f values of valley signify that most of the basins are V-shaped valley which represents a young stage of basin development. A total number of 282 valleys selected for determining the V_f ratio. The thrust passing from V-shaped valleys are more susceptible to the erosional process, and the basins have an active occurrence of landslides and erosional activities. The low V_f values in all basins denote narrow and steep valleys. The higher incision rates and active tectonic uplifts are profound in this type of active basins. The majority of the basins belong to the V-shaped valley (Class 1) while (Class 2) and (Class 3) comprises of wide shape valley (Figure 5b).

4.2.3 Hypsometric curves and Hypsometric Integral

The convex hypsometric curves are characterized by young and slightly eroded regions, S-shaped curves represent moderately eroded regions, and concave shape curves represent highly eroded regions (Pedrera et al. 2009). The concave shape curves are dominant as rocks are eroded,

highly fractured due to structural discontinuities passing through the basins. The range of higher to lower values of hypsometric integral suggests that vast amount of mass is subjected to denudational process while lots of material has been eroded (Hamdouni et al. 2008). The high elevation and low relief surfaces work as a contributing factor towards tectonic disturbances in the basin. The values of hypsometric integral ranges between 0.12 and 0.51 in which higher values signify the convex shape curve while lower values represent a concave shape curve (Figure 6b).

The lower Hi values in the basins resulted due to the high kinetic energy of runoff which dissected the landscape due to high erosional activities (Shukla et al. 2013).

4.2.4 Stream Length Gradient Index

The stream length gradient index and actual river profile indicate that there is an increase in SL index value near tectonically active zones. The SL index values show anomalous behavior when passing through the major thrust such as Ramgarh thrust, Almora thrust, and variable lithological zones. The SL index values calculated for each basin and the majority of the basins were classified in moderately active tectonic zones. Basins belong to highly active tectonic zone (Class 1) consists of 122 km² while moderately active tectonic zone (Class 2) covers 902 km², and 232 km² of the study area belongs to Class 3 (low tectonically active zone). The basins with higher tectonic activity have two major faults passing through them. The basins with lower SL index values have variable lithological contrast and tectonic disturbances within formations. The basin in the north-west portion belongs to class 2 of the moderately tectonic active zone. The higher SL values over variable lithology and thrusts signify tectonic control (Sharma et al. 2018). The lower values of SL index represent when streams are flowing through strike-slip faults (Dehbozorgi et al. 2010). There are contrast views regarding an increase in SL index values concerning variable lithology and tectonic activities. (Harkins et al. 2005) suggested that SL index values increases in more resistant bedrock. However, (Brookfield 1998) suggested that tectonic activities cause higher SL index values. The increase in SL values of this study area resulted from tectonic disturbances as well as

lithological contrast (Figure 7a and 7b).

4.2.5 Basin shape and Mountain front Sinuosity Index

Basin shape index was interpreted to determine the influence of tectonic activity. The elongated basins are covering an area of 445 km² while the rest of the basin area comes under moderate (352 km²) and less (460 km²) tectonically active basin (Figure 8a). The mountain front sinuosity Index with higher tectonic activity covers an area of 555 km². The elongated basin portion belongs to Almora thrust zone (Figure 8b).

4.3 Cumulative analysis of Linear, Areal, Relief and Geomorphic Indices and its validation

The parameters and indices categorized into different classes based on previous literature and K-means clustering as represented in (Appendix 5). The average of linear, areal and relief parameters and geomorphic indices were used to evaluate the spatial distribution of relative tectonic activity of

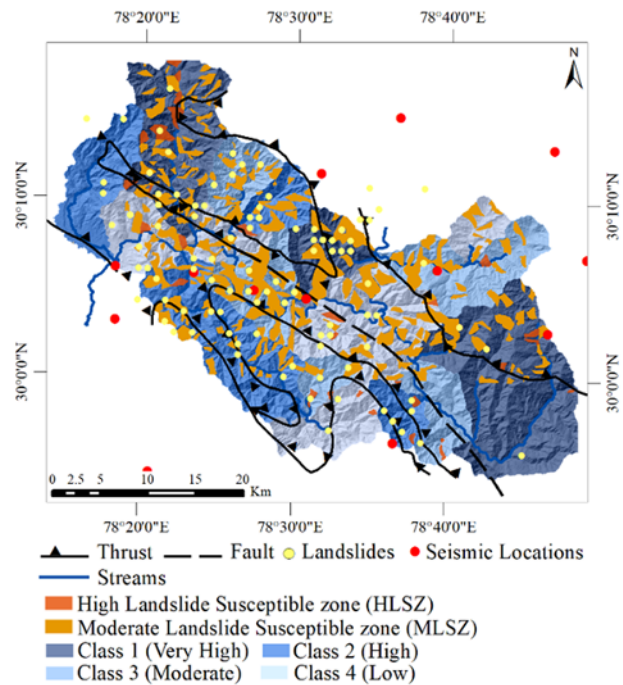


Figure 9 Final distribution of Relative tectonic activity index (I_{at}) with the distribution of landslide, earthquake, and Landslide susceptible zone which represents High Landslide Susceptible Zone (HLSZ), Moderate Landslide Susceptible Zone (MLSZ) and zone except HLSZ and MLSZ comes under Low Landslide Susceptible Zone (LLSZ).

Table 6 Calculation of Relative Tectonic Activity Index (Iat) using Linear, Areal, Relief and Geomorphic Indices as a tool If⁺ = (S/n) , $S = SL + Hi + AF + Bs + V_f + S_{mf}$, Final* = $(If^+ + Avg_{linear} + Avg_{areal} + Avg_{relief})/n$, n = number of parameters, Avg = Average, LAR = Linear, Areal and Relief.

Basin index	Geomorphic indices						If ⁺	LAR parameters			Final*	Iat
	SL	Hi	AF	Bs	V _f	S _{mf}		Avg _{linear}	Avg _{areal}	Avg _{relief}		
1	2	3	3	2	2	1	2.17	2.50	1.50	1.67	1.96	1
2	2	3	3	1	3	3	2.50	2.50	1.33	1.67	2.00	2
3	3	3	3	3	1	2	2.50	3.00	1.83	2.00	2.33	4
4	3	3	2	1	1	2	2.00	2.50	1.33	2.33	2.04	2
5	3	3	2	3	1	2	2.33	2.50	2.17	2.33	2.33	4
6	3	3	3	3	1	1	2.33	2.00	2.33	2.33	2.25	4
7	2	2	2	3	1	2	2.00	2.50	2.67	2.33	2.38	4
8	2	3	3	2	1	2	2.17	3.00	2.17	1.33	2.17	3
9	2	3	3	2	1	1	2.00	3.00	1.83	1.33	2.04	2
10	2	2	2	3	1	1	1.83	3.00	1.67	2.33	2.21	3
11	2	3	1	3	1	3	2.17	2.00	2.33	2.67	2.29	4
12	2	2	3	2	1	1	1.83	2.50	1.67	2.67	2.17	3
13	2	3	1	3	2	3	2.33	3.00	1.83	2.00	2.29	4
14	1	2	3	1	1	1	1.50	2.50	2.00	1.33	1.83	1
15	1	2	2	1	1	2	1.50	1.50	1.67	1.33	1.50	1
16	1	1	3	1	1	1	1.33	2.00	1.83	1.67	1.71	1
17	2	2	3	3	1	1	2.00	3.00	2.00	1.00	2.00	2
18	2	2	1	3	1	2	1.83	3.00	2.50	2.00	2.33	4
19	3	3	1	3	1	2	2.17	2.50	2.67	1.67	2.25	4
20	2	2	3	2	1	1	1.83	3.00	1.67	2.33	2.21	3
21	2	1	3	2	2	1	1.83	2.50	2.00	3.00	2.33	4
22	2	3	3	3	2	1	2.33	2.50	1.83	2.00	2.17	3
23	2	2	1	3	2	3	2.17	3.00	1.83	1.67	2.17	3
24	1	2	1	2	1	1	1.33	3.00	1.67	1.33	1.83	1
25	1	2	2	1	1	1	1.33	2.50	1.67	2.33	1.96	1
26	2	1	1	3	2	1	1.67	2.50	2.17	2.33	2.17	3
27	2	3	3	1	1	2	2.00	2.00	1.33	1.67	1.75	1

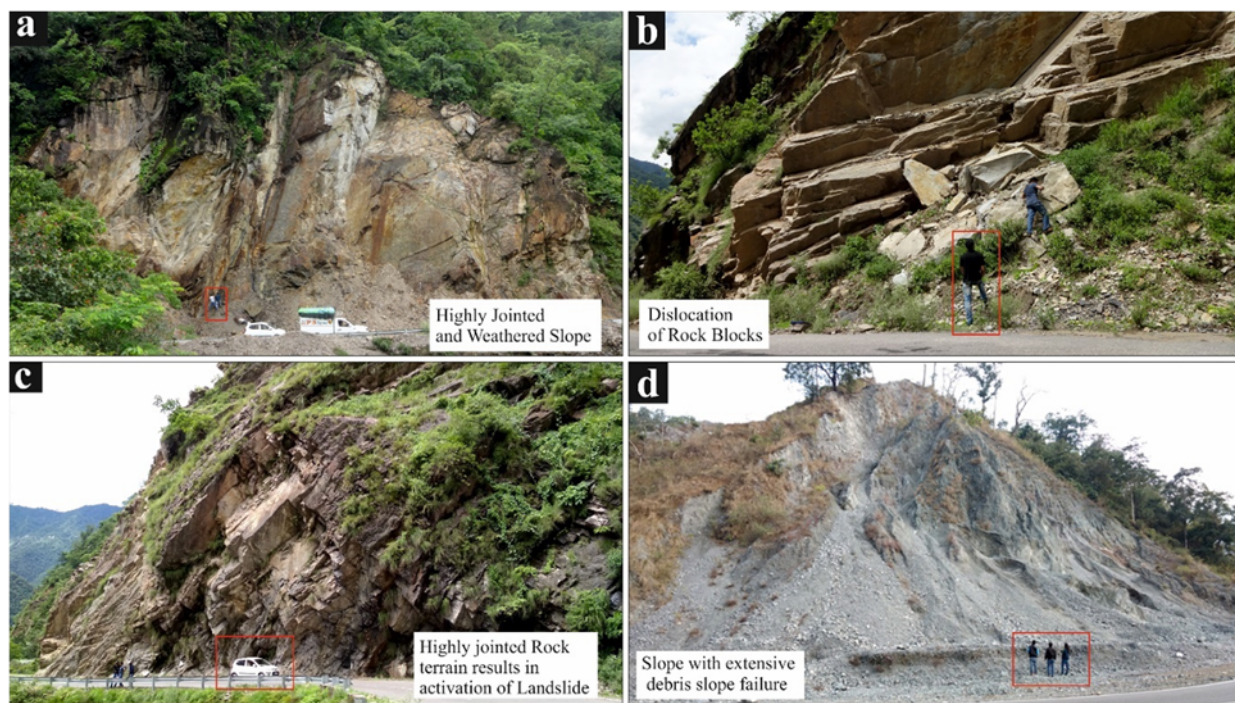


Figure 10 Neotectonics activities in a part of Ganga Basin.

the study area. The values of Relative Tectonic Activity Index were grouped into four classes based on tectonic activity (Hamdouni et al. 2008). The distribution of Iat classes has been classified as Class 1, Very high tectonic activity (<1.97); Class 2, high tectonic activity (1.97 – 2.05); Class 3, Moderate tectonic activity (2.05 – 2.21) and Class 4, Low tectonic activity (> 2.21) based on tectonic activities. The spatial distribution of Final Iat class is represented in (Figure 9 and Table 6). The results interpreted from Iat have been validated with field studies as neotectonics activities resulted in activation of landslides, earthquakes and other natural hazards (Figure 10). These parameters are evaluated to determine the decisive factors for increasing geohazards in the area. The number of landslides occurring along NH -58 (Siddique et al. 2017; Vishal et al. 2017; Siddique and Pradhan 2018) and in adjoining basins correlates with morphometric and geomorphic indices. The landslide susceptibility mapping (GSI 2016) of the Ganga river along NH 58 has a positive relationship with the cumulative result of Iat and morphometric parameters.

5 Conclusion

The role of active tectonics in the part of the Ganga river basin along NH -58 is evident from the evaluated morphometric parameters (Linear, Areal and Relief parameters) and Geomorphic Indices. These parameters have been selected to analyze the occurrence of landslide and neotectonic activities in the region. The incorporation of linear, areal and relief parameters with geomorphic indices act as a

significant tool for Relative Tectonic Activity Index (Iat), as it shows a strong correlation with structural discontinuities and geomorphological anomalies. The approach helps in identification of tectonically active zones. The results of linear, areal and relief parameters have a profound role in active tectonism as major thrust like Berinag thrust, Almora thrust passing through the basins. The calculation of the V_f ratio determines that the majority of basins have a higher tectonic regime. The values of asymmetric factors of different basins define that basins have structural discontinuity and its passing through major faults and thrusts. The Anomalous values Hi , SL index are representative that most of the basins are subjected to active erosional processes or have significant tectonic disturbances. Higher values of B_s and lower values of S_{mf} are also determinant factors for active tectonism in the study area. The combination of all those parameters with linear, areal and relief parameters will help in determining the Iat. The correlation of Iat with landslide susceptibility mapping, field studies and seismic activities have determined the role of active tectonics in occurrences of landslides and other natural hazards. The study will help in determining the actual causative factors for the occurrence of a major disaster like landslide, earthquake, and floods. It will assist in the identification of hazard-prone areas and helps in suggesting suitable remedial measures for mitigation of disasters.

Electronic supplementary material:

Supplementary material (Appendices 1 to 5) is available in the online version of this article at <https://doi.org/10.1007/s11629-018-5172-2>.

References

- Alipoor R, Poorkermani M, Zare M, et al. (2011) Active tectonic assessment around Rudbar Lorestan dam site, High Zagros Belt (SW of Iran). *Geomorphology* 128(1-2): 1-14.
<https://doi.org/10.1016/j.geomorph.2010.10.014>
- Anand AK, Prasad PS, Kumar K (2017) Geomorphometric Analysis of Chamoli and Karnaprayag District, Uttrakhand in Respect to Hazard Zonation of The Area. *Journal of Remote Sensing and GIS* 6(2): 6-11.
<https://doi.org/10.4172/2469-4134.1000202>
- Auden JB (1934) The geology of the Krol Belt. *Records of the Geological Survey of India* 67(4): 357-454.
- Azor A, Keller EA, Yeats RS (2002) Geomorphic indicators of active fold growth: South Mountain–Oak Ridge anticline, Ventura basin, Southern California. *Bulletin of the Geological Society of America* 114(6): 745-753.
[https://doi.org/10.1130/0016-7606\(2002\)114<0745:GIOAFG>2.0.CO;2](https://doi.org/10.1130/0016-7606(2002)114<0745:GIOAFG>2.0.CO;2)
- Bookhagen B, Thiede RC, Strecker MR (2005) Late Quaternary intensified monsoon phases control landscape evolution in the northwest Himalaya. *Geology* 33(2): 149-152.
<https://dx.doi.org/10.1130/G20982.1>
- Brookfield ME (1998) The evolution of the great river systems of southern Asia during the Cenozoic IndiaAsia collision: rivers draining southwards. *Geomorphology* 22(3-4): 285-312.
[https://doi.org/10.1016/S0169-555X\(97\)00082-2](https://doi.org/10.1016/S0169-555X(97)00082-2)
- Bull WB (2007) *Tectonic Geomorphology of Mountain: A New*

- Approach to Paleoseismology.
<https://doi.org/10.1002/9780470692318>
- Bull WB (1978) Geomorphic Tectonic Classes of the South Front of the San Gabriel Mountains, California. U.S. Geological Survey Contract Report, 14-08-001-G-394, Office of Earthquakes, Volcanoes and Engineering, Menlo Park, CA.
- Bull WB, McFadden LD (1977) Tectonic geomorphology north and south of the Garlock Fault, California. Proceedings of the Eighth Annual Geomorphology Symposium, in: Geomorphology in Arid Regions, Doebring, D. O., (Ed), State University of New York, Binghamton 115-138.
- Chen Y, Sung Q, Cheng K (2003) Along-strike variations of morphotectonic features in the Western Foothills of Taiwan : tectonic implications based on stream-gradient and hypsometric analysis. *Geomorphology* 56(1): 109-137.
[https://doi.org/10.1016/S0169-555X\(03\)00059-X](https://doi.org/10.1016/S0169-555X(03)00059-X)
- Cheng Y, He C, Rao G, et al. (2018) Geomorphological and structural characterization of the southern Weihe Graben, central China: Implications for fault segmentation. *Tectonophysics* 722: 11-24.
<https://doi.org/10.1016/j.tecto.2017.10.024>
- Cox RT (1994) Analysis of drainage-basin symmetry as a rapid technique to identify areas of possible Quaternary tilt-block tectonics: an example from the Mississippi Embayment. *Geological Society of America Bulletin* 106(5): 571-581.
[https://doi.org/10.1130/00167606\(1994\)106<0571:AODBSA>2.3.CO;2](https://doi.org/10.1130/00167606(1994)106<0571:AODBSA>2.3.CO;2)
- Dehbozorgi M, Pourkermani M, Arian M, et al. (2010) Geomorphology Quantitative analysis of relative tectonic activity in the Sarvestan area, central Zagros, Iran. *Geomorphology* 121(3): 329-341.
<https://doi.org/10.1016/j.geomorph.2010.05.002>
- Fuchs G, Sinha AS (1974) On the geology of Nanital (Kumaun Himalaya). *Himalayan Geology* 4: 563-580.
- Gaidzik K, Ramírez-Herrera MT (2017) Geomorphic indices and relative tectonic uplift in the Guerrero sector of the Mexican forearc. *Geoscience Frontiers* 8(4): 885-902.
<https://doi.org/10.1016/j.gsf.2016.07.006>
- Ghosh B, Pappin JW, So MML, et al. (2012) Seismic hazard assessment in India. Proceedings of the Fifteenth World Conference on Earthquake Engineering, Lisbon, Portugal.
- GSI (2016) Landslide compendium of North west Himalaya, special publication no. 107, ISSN: 0254-0436.
- Hack JT (1973) Stream-profile analysis and stream-gradient index. *Journal of Research of the U.S. Geological Survey* 1(4): 421-429. <http://pubs.er.usgs.gov/publication/70161653>
- Hare PW, Gardner TW (1985) Geomorphic indicators of vertical neotectonism along converging plate margins, Nicoya Peninsula, Costa Rica. *Binghamton Symposia in Geomorphology: International Series* 15: 75-104.
- Hamdouni R El, Irigaray C, Fernández T, et al. (2008) Assessment of relative active tectonics, southwest border of the Sierra Nevada (southern Spain). *Geomorphology* 96(1-2): 150-173. <https://doi.org/10.1016/j.geomorph.2007.08.004>
- Harkins NW, Anastasio DJ, Pazzaglia FJ (2005) Tectonic geomorphology of the Red Rock fault, insights into segmentation and landscape evolution of a developing range front normal fault. *Journal of Structural Geology* 27(11): 1925-1939. <https://doi.org/10.1016/j.jsg.2005.07.005>
- Horton, RE (1945) Erosional development of streams and their drainage basins: hydrophysical approach to quantitative morphology. *GSA Bulletin* 56(3): 275-370.
[https://dx.doi.org/10.1130/0016-7606\(1945\)56\[275:EDOSAT\]2.0.CO;2](https://dx.doi.org/10.1130/0016-7606(1945)56[275:EDOSAT]2.0.CO;2)
- Hurtrez JE, Sol C, Lucaleau F (1999) Effect of drainage area on hypsometry from an analysis of small-scale drainage basins in the siwalik hills (Central Nepal). *Earth Surface Processes and Landforms* 24(9): 799-808.
[https://doi.org/10.1002/\(SICI\)1096-9837\(199908\)24:9<799::AID-ESP12>3.0.CO;2-4](https://doi.org/10.1002/(SICI)1096-9837(199908)24:9<799::AID-ESP12>3.0.CO;2-4)
- ISC (2016) International Seismological Centre, On-line Bulletin, <http://www.isc.ac.uk>, International Seismological Centre
- Thatcham, United Kingdom.
<http://doi.org/10.31905/D8o8B830>
- Joshi LM, Kotlia BS (2015) Neotectonically triggered instability around the palaeolake regime in Central Kumaun Himalaya, India. *Quaternary International* 37: 219-231.
<https://doi.org/10.1016/j.quaint.2014.10.033>
- Keller EA, Pinter N (Eds.) (2002) Active Tectonics: Earthquakes, Uplift, and Landscape, 2nd ed. Prentice Hall, Upper Saddle River, NJ. p. 362
- Keller EA, Pinter N (1996) Active Tectonics: Earthquake, Uplift, and Landscape. Prentice Hall, Upper Saddle River, NJ. p. 338
- Keller EA (1986) Investigation of active tectonics: use of surficial earth processes. In: Wallace, R.E. (Ed.), Active Tectonics, Studies in Geophysics. National Academy Press, Washington, DC. 136-147
- Mahmood SA, Gloaguen R (2012) Appraisal of active tectonics in Hindu Kush: Insights from DEM derived geomorphic indices and drainage analysis. *Geoscience Frontiers* 3(4): 407-428. <https://doi.org/10.1016/j.gsf.2011.12.002>
- Manu MS, Anirudhan S (2008) Drainage characteristics of Achankovil River Basin, Kerala. *Journal of Geological Society of India* 71(6): 841-850
<http://www.geosocindia.org/index.php/jgsi/article/view/80780>
- Mayer L (1990) Introduction to Quantitative Geomorphology. Prentice Hall, Englewood, Cliffs, NJ.
- Ozdemir H, Bird D (2009) Evaluation of morphometric parameters of drainage networks derived from topographic maps and DEM in point of floods. *Environmental Geology* 56(7): 1405-1415.
<https://doi.org/10.1007/s00254-008-1235-y>
- Pazzaglia FJ (2013) 9.22 Fluvial Terraces. Treatise on Geomorphology. Elsevier, Academic Press 379-412.
<https://doi.org/10.1016/B978-0-12-374739-6.00248-7>
- Pedrera A, Pérez-Peña JV, Galindo-Zaldívar J, et al. (2009) Testing the sensitivity of geomorphic indices in areas of low-rate active folding (eastern Betic Cordillera, Spain). *Geomorphology* 105(3): 218-231.
<https://doi.org/10.1016/j.geomorph.2008.09.026>
- Pérez-Peña JV, Azor A, Azañón JM, et al. (2010) Active tectonics in the Sierra Nevada (Betic Cordillera, SE Spain): Insights from geomorphic indexes and drainage pattern analysis. *Geomorphology* 119(1): 74-87.
<https://doi.org/10.1016/J.GEOMORPH.2010.02.020>
- Pike RJ, Wilson, SE (1971) Elevation relief ratio, hypsometric integral and geomorphic area-altitude analysis. *GSA Bulletin* 82(4): 1079-1084.
[https://dx.doi.org/10.1130/0016-7606\(1971\)82\[1079:ERHIAG\]2.0.CO](https://dx.doi.org/10.1130/0016-7606(1971)82[1079:ERHIAG]2.0.CO)
- Ramírez-Herrera MT (1998) Geomorphic assessment of active tectonics in the acambay graben, Mexican volcanic belt. *Earth Surface Processes and Landforms* 23(4): 317-332.
[https://doi.org/10.1002/\(SICI\)1096-9837\(199804\)23:4<317::AID-ESP845>3.0.CO;2-V](https://doi.org/10.1002/(SICI)1096-9837(199804)23:4<317::AID-ESP845>3.0.CO;2-V)
- Schumm SA (1956) Evolution of drainage systems and slopes in badlands at Perth Amboy, New Jersey. *Bulletin of Geological Society of America* 67(5): 597-646.
[https://doi.org/10.1130/0016-7606\(1956\)67\[597:EODSAS\]2.0.CO;2](https://doi.org/10.1130/0016-7606(1956)67[597:EODSAS]2.0.CO;2)
- Sharma G, Champati ray PK, Mohanty S (2018) Morphotectonic analysis and GNSS observations for assessment of relative tectonic activity in Alaknanda basin of Garhwal Himalaya, India. *Geomorphology* 301: 108-120.
<https://doi.org/10.1016/j.geomorph.2017.11.002>
- Shukla DP, Dubey CS, Ningreichon AS, et al. (2013) GIS-based morpho-tectonic studies of Alaknanda river basin: a precursor for hazard zonation. *Natural Hazards* 71(3): 1433-1452.
<https://doi.org/10.1007/s11069-013-0953-y>
- Siddique T, Pradhan SP, Vishal V, et al. (2017) Stability assessment of Himalayan road cut slopes along National Highway 58, India. *Environmental Earth Sciences* 76(22): 759.
<https://doi.org/10.1007/s12665-017-7091-x>

- Siddique T, Pradhan SP (2018) Stability and sensitivity analysis of Himalayan road cut debris slopes: an investigation along NH-58, India. *Natural Hazards* 93(2): 577-600.
<https://doi.org/10.1007/s11069-018-3317-9>
- Silva PG, Goy JL, Zazo C, et al. (2003). Fault generated mountain fronts in southeast Spain: Geomorphologic assessment of tectonic and earthquake activity. *Geomorphology* 50(1): 203-225.
[https://doi.org/10.1016/S0169-555X\(02\)00215-5](https://doi.org/10.1016/S0169-555X(02)00215-5)
- Singh O, Sarangi A, Sharma MC (2008) Hypsometric integral estimation methods and its relevance on erosion status of North-Western Lesser Himalayan watersheds. *Water Resources Management* 22(11): 1545-1560.
<https://doi.org/10.1007/s11269-008-9242-z>
- Smith JS, Chandler J, Rose J (2009) High spatial resolution data acquisition for the geosciences: kite aerial photography. *Earth Surface Processes and Landforms* 34(1): 155-161.
<https://doi.org/10.1002/esp>
- Sreedevi PD, Owais S, Khan HH, et al. (2009) Morphometric Analysis of a Watershed of South India Using SRTM Data and GIS. *Journal of the Geological Society of India* 73(4): 543-552.
<https://doi.org/10.1007/s12594-009-0038-4>
- Sreedevi PD, Subrahmanyam K, Ahmed S (2005) The significance of morphometric analysis for obtaining groundwater potential zones in a structurally controlled terrain. *Environmental Geology* 47(3): 412-420.
<https://doi.org/10.1007/s00254-004-1166-1>
- Strahler AN (1964) Quantitative geomorphology of drainage basins and channel networks, Hand book of Applied Hydrology, Mc Graw Hill, New York. pp 439-476.
- Strahler AN (1957) Quantitative analysis of watershed geomorphology. *Eos, Transactions American Geophysical Union* 38(6): 913-920.
<https://doi.org/10.1029/TR038i006p00913>
- Strahler AN (1952) Hypsometric (area-altitude) analysis of erosional topography. *Geological Society of America Bulletin* 63(11): 1117-1142.
<https://dx.doi.org/10.1130/0016->
7606(1952)63[1117:HAAOET]2.0.CO.
- Topal S (2018) Quantitative analysis of relative tectonic activity in the Acigöl fault, SW Turkey. *Arabian Journal of Geosciences* 11(9): 198. <https://doi.org/10.1007/s12517-018-3545-z>
- Topal S, Keller E, Bufo A, et al. (2016) Tectonic geomorphology of a large normal fault: Akşehir fault, SW Turkey. *Geomorphology* 259: 55-69.
<https://doi.org/10.1016/j.geomorph.2016.01.014>
- USGS (2018) USGS earthquake data, Earthquake data. <https://earthquake.usgs.gov/data/> (Accessed 15 July 2018)
- Valdiya K (2003) Reactivation of Himalayan Frontal Fault: Implications. *Current Science* 85(7): 1031-1040.
<http://www.jstor.org/stable/24108786>
- Valdiya K (1993) Uplift and geomorphic rejuvenation of the Himalaya in the Quaternary period. *Current Science* 64(11/12): 873-885.
<http://www.jstor.org/stable/24096201>
- Valdiya KS (1980) Geology of Kumaun Lesser Himalaya. Wadia Institute of Himalayan Geology, Publication, Dehradun, 291
- Valdiya KS (1976) Himalayan Transverse Faults and Folds and Their Parallelism with Subsurface Structures of North Indian Plains. *Tectonophysics* 32(3-4): 353-386.
[https://doi.org/10.1016/0040-1951\(76\)90069-X](https://doi.org/10.1016/0040-1951(76)90069-X)
- Valdiya KS (1965) Petrography and sedimentary zone of southern Pithoragarh, U.P. Himalaya. D.N. Wadia Commemorative volume Mining, Geological and Metallurgical Institute of India, Calcutta. 521-544.
- Vishal V, Siddique T, Purohit R, et al. (2017) Hazard assessment in rockfall-prone Himalayan slopes along National Highway-58, India: rating and simulation. *Natural Hazards* 85(1): 487-503. <https://doi.org/10.1007/s11069-016-2563-y>
- Yin A (2006) Cenozoic tectonic evolution of the Himalayan orogen as constrained by along-strike variation of structural geometry, exhumation history, and foreland sedimentation. *Earth-Science Reviews* 76(1): 1-131.
<https://doi.org/10.1016/j.earscirev.2005.05.004>